

**Stabilization of ferrielectric phase in NaNbO₃-based lead-free ceramics for
wide-temperature large electrocaloric effect**

Jie Wu ^{a,b,c}, Hui Liu ^{a,c}, He Qi ^{a,b,c*}, Botao Gao ^{a,b}, Liang Chen ^{a,b}, Wenchao Li ^{a,b},

Shiqing Deng ^{a,c}, and Jun Chen ^{a,b,c*}

^a Beijing Advanced Innovation Center for Materials Genome Engineering, University
of Science and Technology Beijing, Beijing 100083, China.

^b Department of Physical Chemistry, University of Science and Technology Beijing,
Beijing 100083, China

^c School of Mathematics and Physics, University of Science and Technology Beijing,
Beijing 100083, China.

*Corresponding authors: qicheustb@ustb.edu.cn; junchen@ustb.edu.cn

Jie Wu and Hui Liu contributed equally to this work.

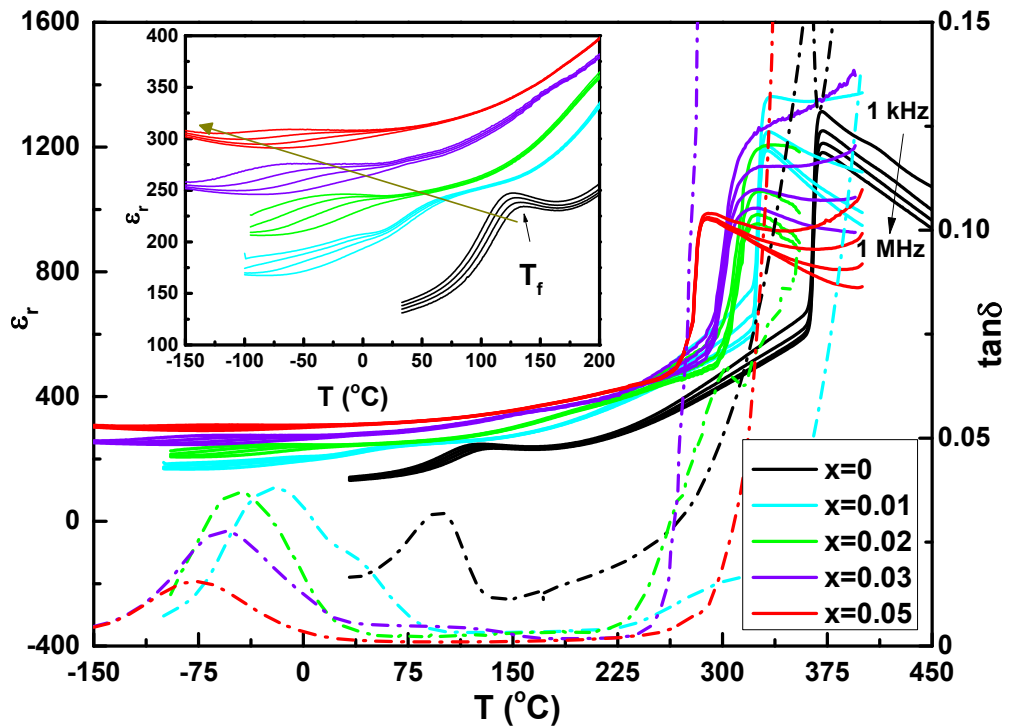


Fig. S1 Temperature dependent dielectric permittivity and dielectric loss at the frequency of 1 kHz-1 MHz for the NN-CZ ceramics. The inset is the evolution of T_f with changing CZ content.

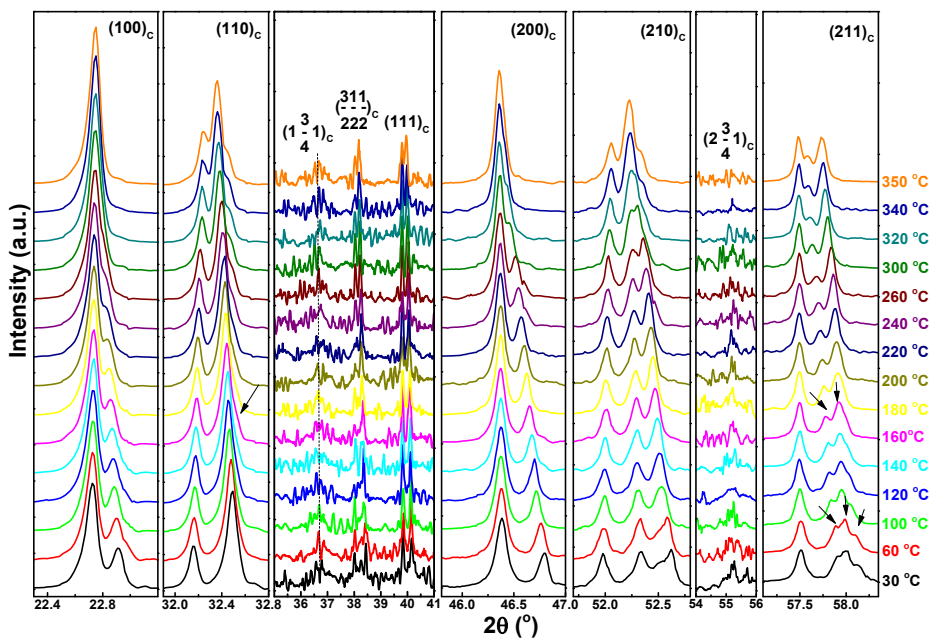


Fig. S2 Temperature-dependent XRD pattern of the NN sample.

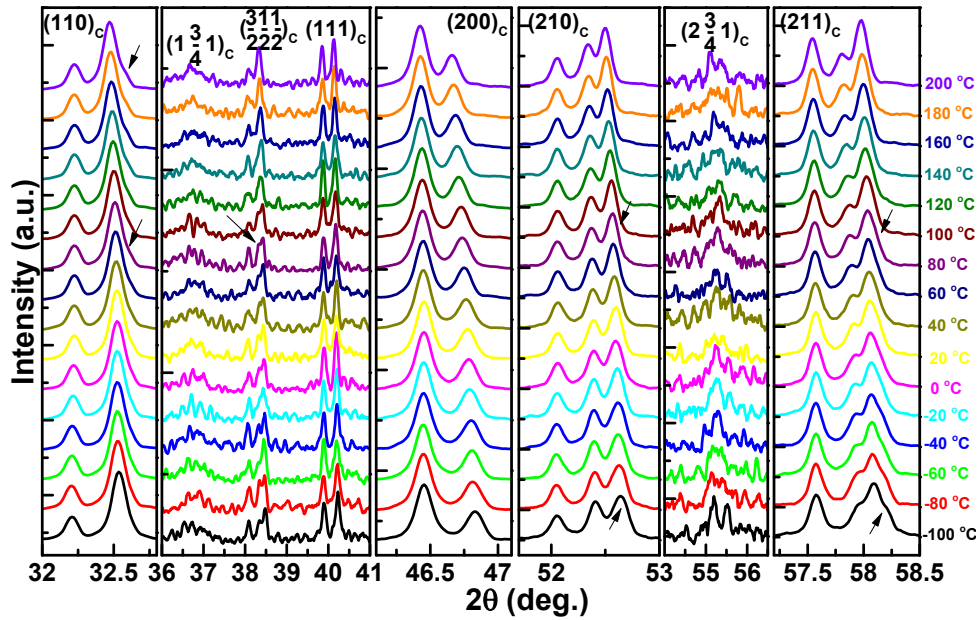


Fig. S3 Temperature-dependent XRD pattern of the NN-0.01CZ sample.

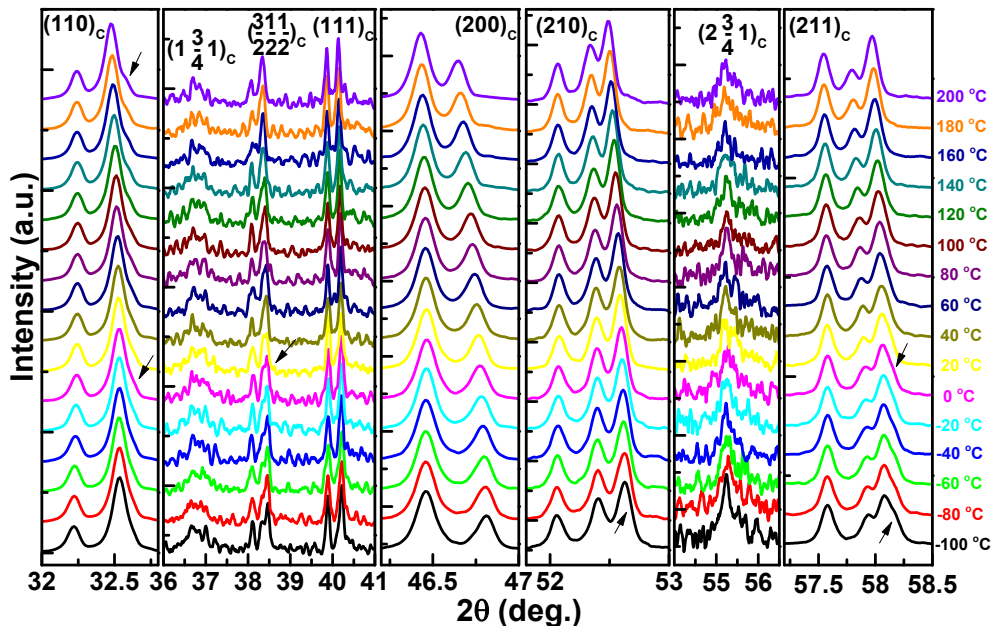


Fig. S4 Temperature-dependent XRD pattern of the NN-0.02CZ sample.

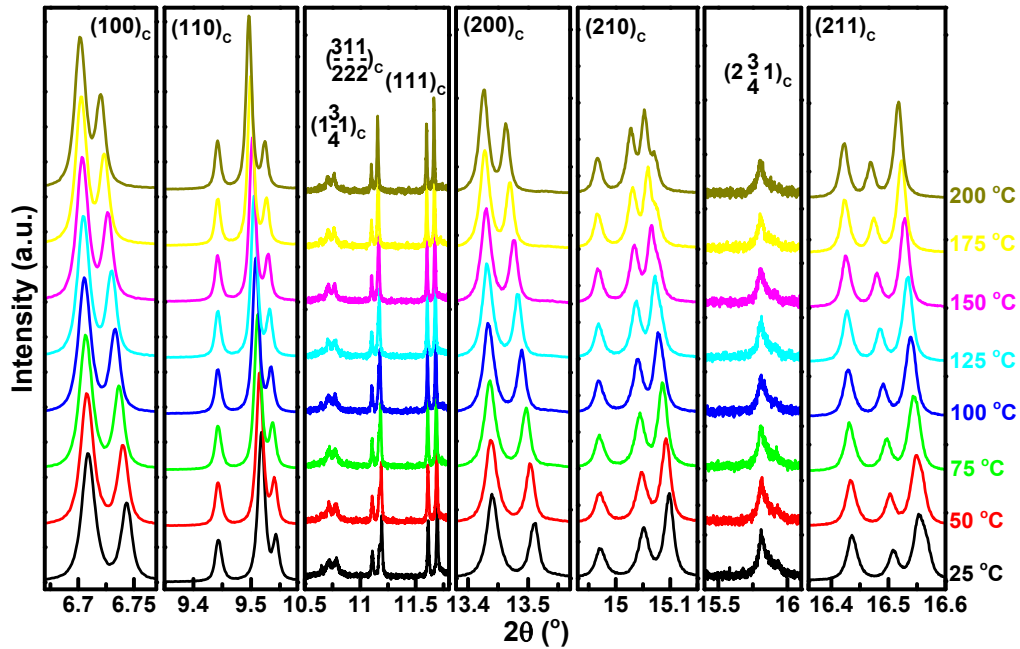


Fig. S5 Temperature-dependent synchrotron XRD pattern of the NN-0.02CZ sample.

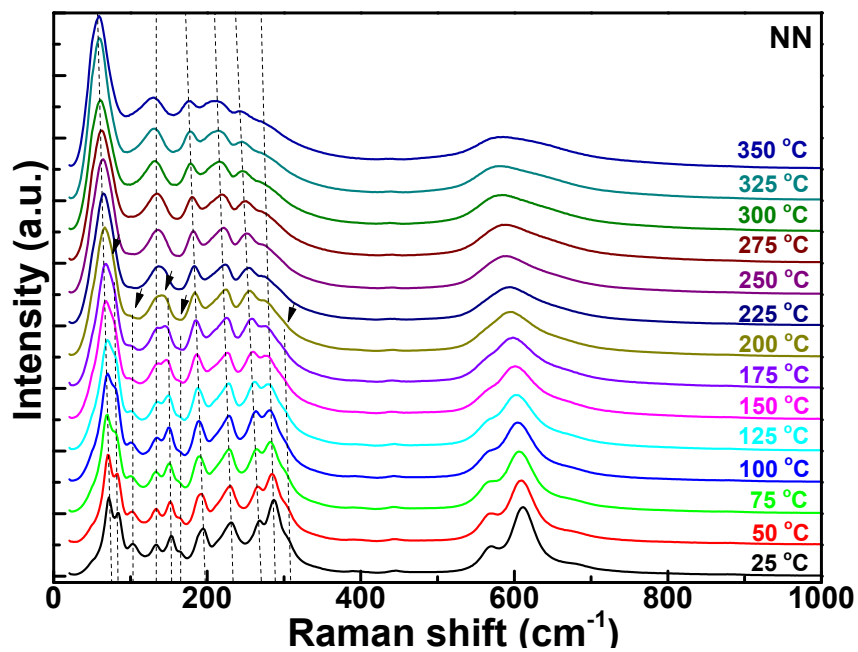


Fig. S6. Temperature-dependent Raman spectra of NN sample.

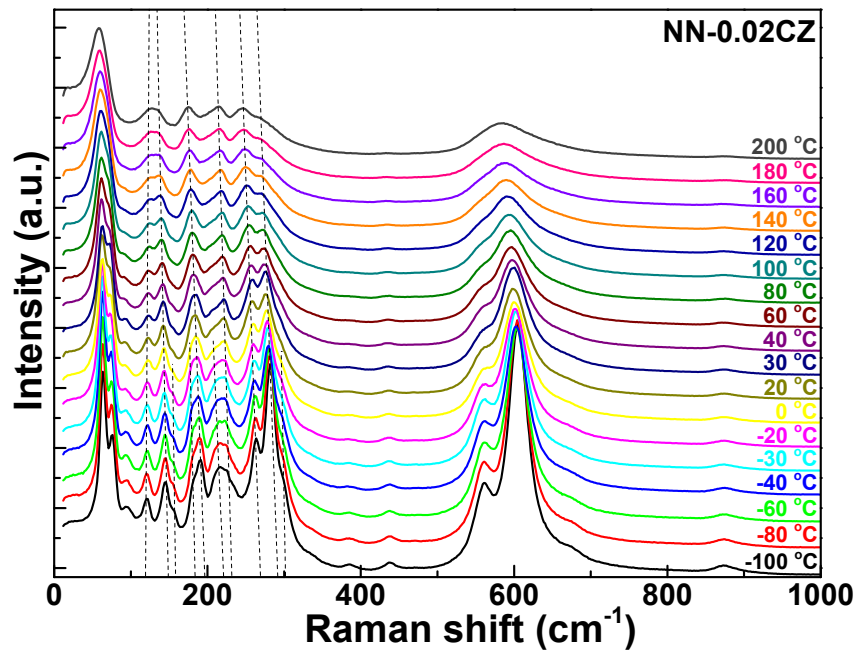


Fig. S7. Temperature-dependent Raman spectra of NN-0.02CZ sample.

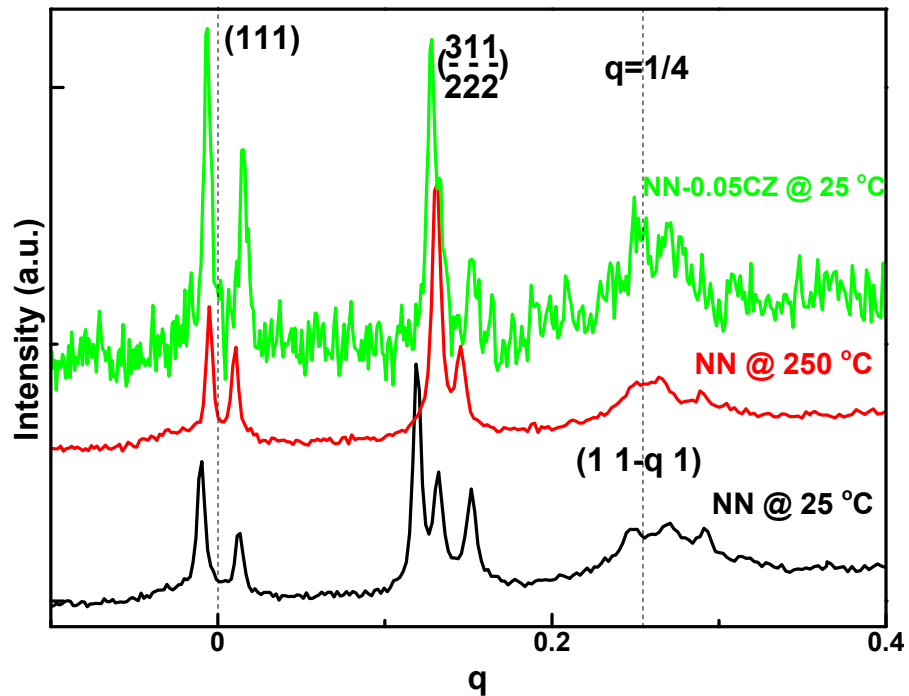


Fig. S8. The corresponding intensity profiles of $(1, 1-\mathbf{q}, 1)$ superlattice reflections and (111) basic reflections for NN-xCZ ceramics.

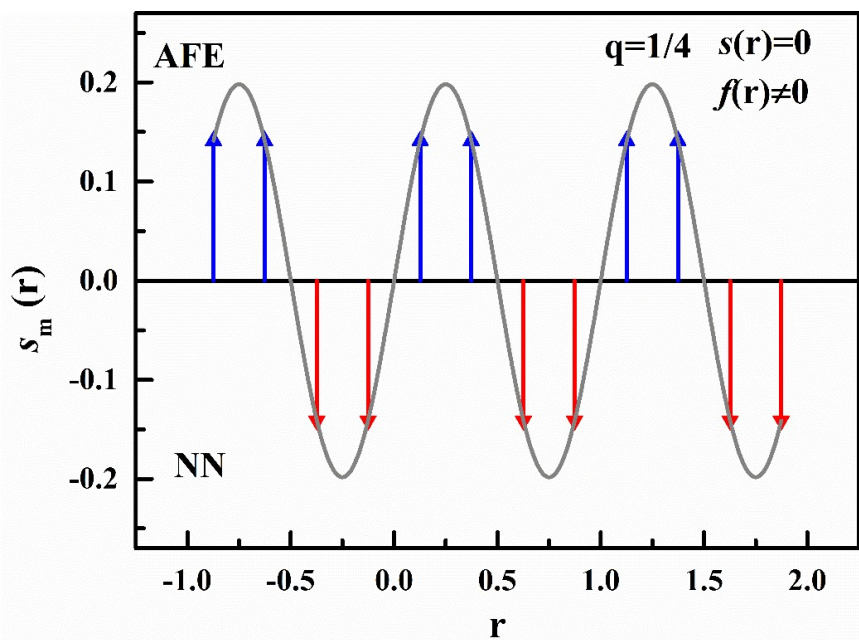


Fig. S9 The proposed configuration for $q=1/4$ phase of NN ceramic.

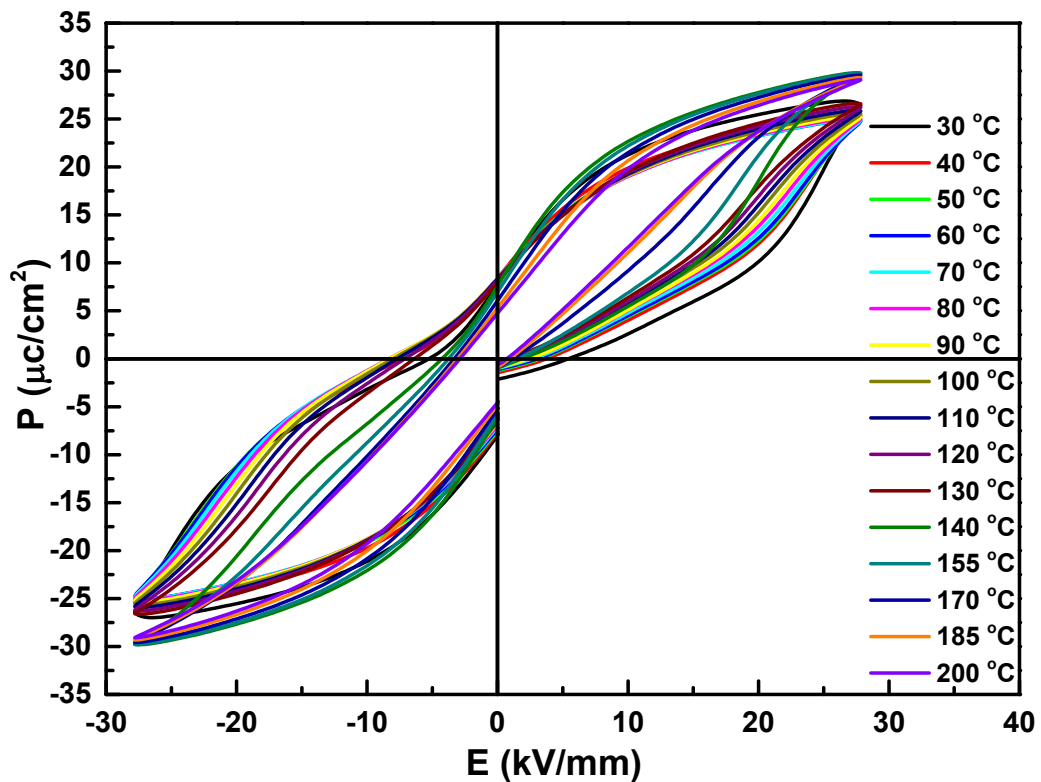


Fig. S10 Temperature-dependent P-E hysteresis loops at 10 Hz of the NN-0.05CZ sample.

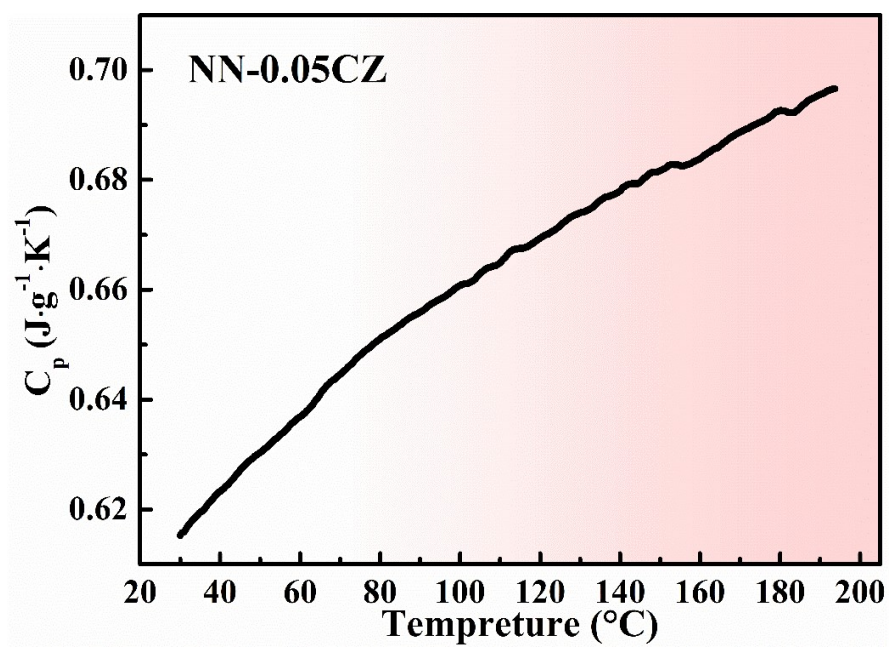


Fig. S11 Temperature dependence of the specific heat curve for the NN-0.05CZ ceramic.

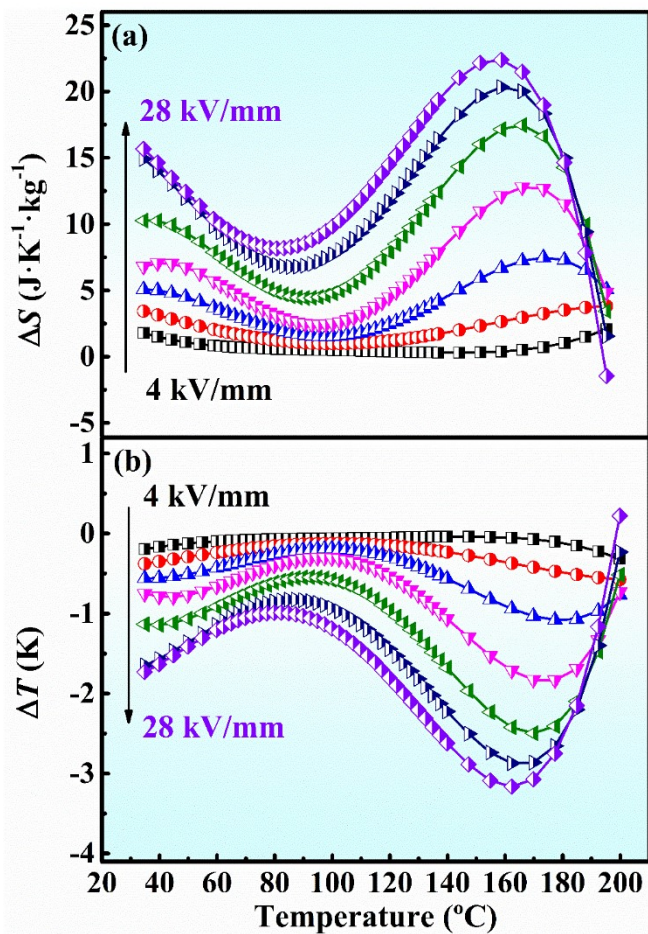


Fig. S12 The ECE (a) ΔS and (b) ΔT for the NN-0.05CZ sample under different applied fields, which exhibits excellent ECE compared with other lead-free ceramics.¹⁻⁷

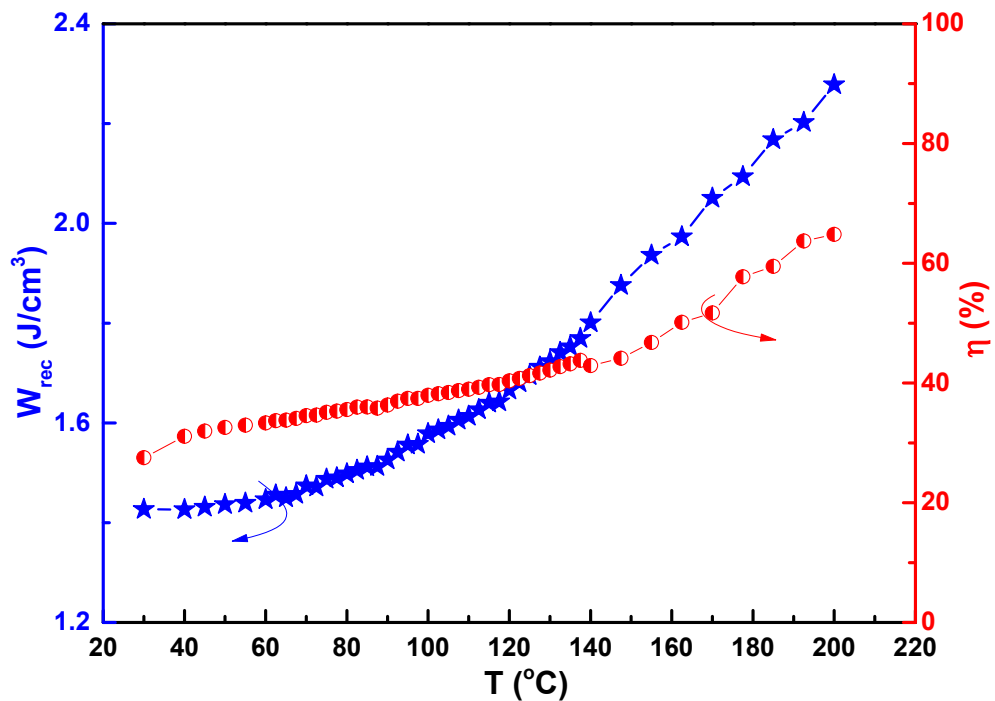


Fig. S13 The temperature dependent recoverable energy storage density W_{rec} and efficiency η of the NN-0.05CZ ceramic.

W_{rec} and η can be calculated as follows:

$$W_{\text{rec}} = \int_{P_r}^{P_{\max}} E \, dP$$

$$W_{\text{total}} = \int_0^{P_{\max}} E \, dP$$

$$\eta = W_{\text{rec}} / W_{\text{total}}$$

where P_{\max} , P_r , E and W_{total} are the maximum polarization, remanent polarization, applied electric field and total energy density.

■ References

- 1 F. Li, K. Li, M. S. Long, C. C. Wang, G. H. Chen and J. W. Zhai, *Appl. Phys. Lett.*, 2021, **118**, 043902.
- 2 Z. Hanani, S. Merselmiz, D. Mezzane, M. Amjoud, A. Bradesko, B. Rozic, M. Lahcini, M. El Marssi, A. V. Ragulya, I. A. Luk'yanchuk, Z. Kutnjak and M. Goune, *RSC Adv.*, 2020, **10**, 30746-30755.
- 3 F. Han, Y. Bai, L. J. Qiao and D. Guo, *J. Mater. Chem. C*, 2016, **4**, 1842-1849.
- 4 Q. M. Wei, M. K. Zhu, M. P. Zheng, Y. D. Hou, J. J. Li and Y. Bai, *Scripta Mater.*, 2019, **171**, 10-15.
- 5 J. T. Li, Y. Bai, S. Q. Qin, J. Fu, R. Z. Zuo and L. J. Qiao, *Appl. Phys. Lett.*, 2016, **109**, 162902.
- 6 X. J. Jiang, L. H. Luo, B. Y. Wang, W. P. Li and H. B. Chen, *Ceram. Int.*, 2014, **40**, 2627-2634.
- 7 X. J. Wang, J. G. Wu, B. Dkhil, B. X. Xu, X. P. Wang, G. H. Dong, G. Yang and X. J. Lou, *Appl. Phys. Lett.*, 2017, **110**, 063904.